Jpn. J. Appl. Phys. Vol. 33 (1994) pp. L 1301–L 1303
Part 2, No. 9B, 15 September 1994

Superparamagnetic Nanocomposite of Silver/Iron-Oxide by Inert Gas Condensation

Takao YAMAMOTO[*1,*2], Robert D. SHULL[1], Prabhakar R. BANDARU[2], Frederic COSANDEY[2] and Horst W. HAHN[3]

Research Institute for Advanced Science and Technology, University of Osaka Prefecture, 1-2 Gakuen, Sakai, Osaka 593
[1]*Magnetic Materials Group, National Institute of Standard and Technology, Gaithersburg, MD 20899, USA*
[2]*Department of Materials Science and Engineering, Rutgers University, Piscataway, NJ 08855, USA*
[3]*Materialwissenschaft, Technische Hochschule Darmstadt, 64295 Darmstadt, Germany*

(Received July 15, 1994; accepted for publication August 20, 1994)

A superparamagnetic nanocomposite of silver and iron oxide was synthesized by gas condensation. The procedure involved (1) coevaporation of silver and iron, (2) *in situ* oxidation of iron particles, (3) *in situ* compaction, and (4) post-annealing in an inert or an oxidizing atmosphere. The magnetization plots against H/T fell on a single curve from room temperature to 160 K, thereby providing evidence of superparamagnetism. Annealing treatment modifies the effective magnetic moment size and saturation value of magnetization. The present process is a potential synthesis route for magnetic nanocomposites useful for applications such as magnetic refrigeration, recording and permanent magnets.

KEYWORDS: nanocomposite, nanocrystals, superparamagnetism, iron oxide, silver, inert gas condensation, magnetic materials, magnetization, giant magnetoresistance, magnetic refrigeration

1. Introduction

Recently material scientists have paid much attention to nanocomposites in which magnetic nanoparticles are dispersed in a nonmagnetic matrix, because of numerous interesting and important science and technology aspects.[1,2] For example, the technologically important phenomenon of giant magnetoresistance (GMR) was found in granular type nanocomposites[3-5] as well as in layered type structures. Consequently much emphasis is now being directed to synthesize materials with better GMR performance and to understand its mechanism. Another challenge is the synthesis of nanocomposites for magnetic refrigeration based on a prediction that these materials could be operated at higher temperatures and with an efficiency higher than those available today.[6-8]

In this paper, we report on the synthesis of a superparamagnetic nanocomposite of magnetic iron oxide and silver by a gas condensation method combined with post annealing treatment of the compacted samples. The observation of superparamagnetic iron-oxide grains in a metallic silver matrix suggests the possibility of the occurance of GMR in these samples and the usefulness of these materials for magnetic refrigeration applications. In this paper, we focus on material processing aspects and measurements of magnetization behavior. Detailed results on materials evaluation will be reported elsewhere. Gas condensation processing[9] was chosen for its versatility and flexibility in modification of synthesis parameters.

2. Experimental

The samples were synthesized by the inert gas condensation technique. Metallic iron and silver were evaporated from resistance heated boats in a chamber filled with helium gas of 7×10^2 Pa. The helium gas quenches the vapor, and nanoparticles are formed above the boats and transported to the surface of a particle collector cooled by liquid nitrogen. The collector is cylindrical and rotates during the evaporation process to obtain a homogeneous mixture of the two species. After evaporation, only the iron particles are oxidized by oxygen gas exposure up to 40 Pa. Subsequently, the silver and iron-oxide powder mixture is scraped off the collector surface and transported *in situ* to a chamber for compaction. The compaction conditions are 275 MPa at room temperature. One of the samples was annealed in an inert atmosphere of helium at 250°C for 1 h, while another was annealed in an oxidizing atmosphere of 10%-O_2/He at 230°C for 15 h. A small amount of loose powder was collected for transmission electron microscopy (TEM). The iron concentration was determined by Rutherford backscattering spectroscopy (RBS). Sizes of primary particles in the loose powder and of grains in the compacted pellets are evaluated by high resolution TEM (HRTEM) assisted by selected area electron diffraction (SAD), energy disperse fluorescence X-ray spectroscopy (EDX) and an image analysis system with a fast Fourier transform (FFT). Mössbauer and X-ray absorption spectroscopy (XAS) were employed for the phase identification. The XAS measurements were done at the Brookhaven National Synchrotron Light Source on beamline X-19A. The magnetization was measured by a vibrating sample magnetometer at various temperatures.

3. Results and Discussion

Figure 1 shows a TEM micrograph of the as-prepared loose powder. From the uniformity for the two constituants it is concluded that sizes and shapes of iron oxide and silver nanoparticles are not significantly different. This is further supported by dark field electron microscopy. Figure 2 shows a HRTEM micrograph of the as-compacted pellet showing lattice fringes, indicating that the particles are crystalline and defect free. The EDX and FFT techniques make it possible to distinguish between grains of iron oxide and silver and to estimate the size of each species. Table I summarizes the sizes. The grain growth due to the annealing processes is found to be less than a factor of two.

*[1]visited Rutgers Univ. and NIST.
*[2]E-mail address: takao@center.osakafu-u.ac.jp

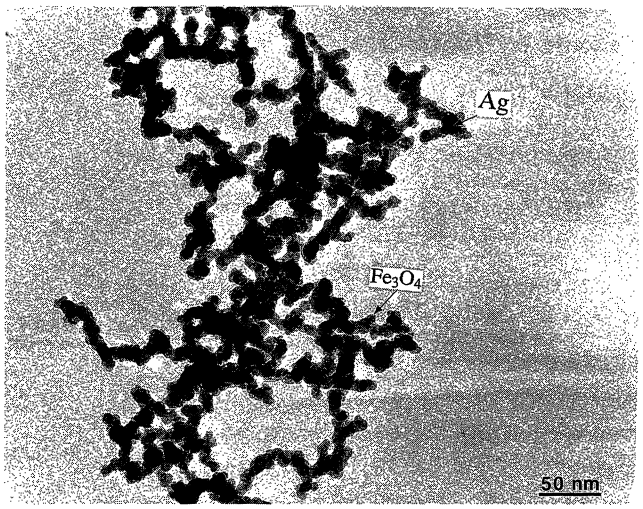

Fig. 1. A TEM micrograph of loose powder of Ag/FeO_x nanocomposite containing 40 at% iron.

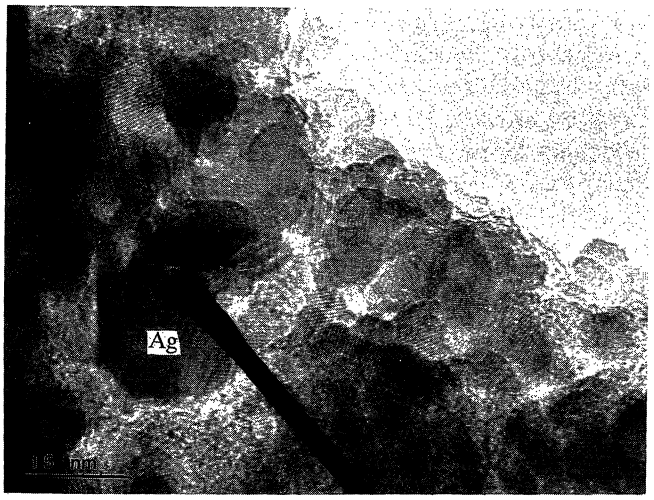

Fig. 2. A HRTEM micrograph of the as-compacted Ag/FeO_x nanocomposite containing 40 at% iron.

Results on identification of iron oxide phases are summarized in Table II. Detailed results will be presented elsewhere. Silver was found to exist as metal by X-ray diffraction and silver-L-edge XAS measurement.

Figure 3 shows the magnetization data of three samples, as-compacted, He-annealed and O_2-annealed, all of which were made from a batch of powder containing 40 at% of iron. In the figure, the magnetization M is plotted versus $\mu_B H/T$, where μ_B is the Bohr magneton, H the applied magnetic field, and T is the temperature. The data points of all samples fall all collapse onto a single curve from 160 K to 290 K, providing evidence for the occurrence of superparamagnetism.[10] At temperatures below this range, the plots exhibit a remanence and a deviation from the curve, indicating interactions between magnetic particles.

Table I. Sizes of particles and grains of Ag/FeO_x nanocomposite containing 40 at% iron estimated by TEM (nm).

	Loose powder	As-compacted	He-annealed[a)]	O_2-annealed[b)]
Ag	15	25	30	35
FeO_x	15	15	20	20

[a)]in He at 250°C for 1 h, [b)]in 10%O_2/He at 230° for 15 h.

Table II. Iron oxide phases in Ag/FeO_x nanocomposite detected by various methods.

Method	Loose powder	As-compacted	He-annealed	O_2-annealed
SAD	Fe_3O_4	Fe_3O_4 +γ-Fe_2O_3	γ-Fe_2O_3	γ-Fe_2O_3
Mössbauer	Fe_3O_4+Fe	—	—	—
XAS	—	Fe_3O_4+Fe +γ-Fe_2O_3	γ-Fe_2O_3	γ-Fe_2O_3

"—" means "not measured".

In the figure, two points should be noted. One is that two of these samples, as-compacted and He-annealed, exhibit remanences M_R, though small, while the O_2-annealed one exhibits none as shown in an inset in Fig. 3. The other feature is that their saturation magnetizations σ_s are in the order of

$$\sigma_s(\mathrm{He}) > \sigma_s(\mathrm{AsC}) >> \sigma_s(\mathrm{O_2}).$$

These two points can be interpreted as follows. In the as-compacted material, a part of iron (or iron oxide) exists in the silver matrix as clusters that are too small to give rise to ferri- or ferromagnetism. The annealing process induces growth to a size supporting magnetism, causing an increase of σ_s. The O_2 annealing process induces a part of the iron species to form an antiferromagnetic phase, α-Fe_2O_3. This phase not only reduces σ_s but also

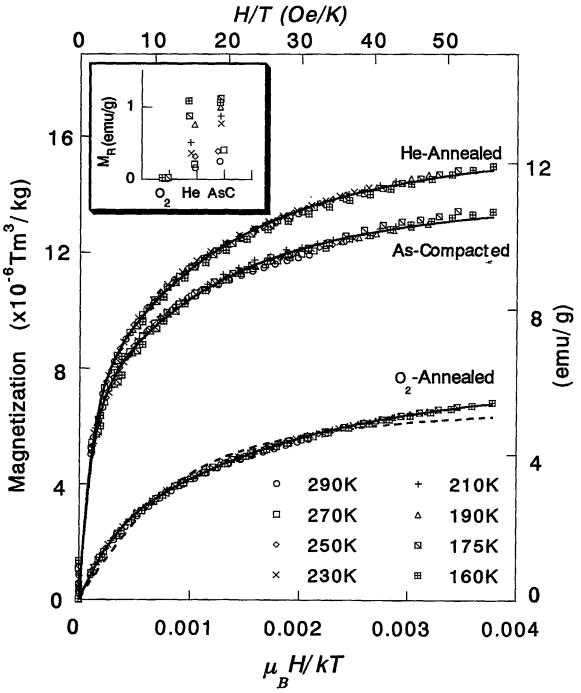

Fig. 3. Magnetization of as-compacted and heat treated nanocomposites of Ag/FeO_x containing 40 at% iron at various temperatures. Dashed and solid curves indicate fitting results assuming a simple and a bimodal Langevin function, respectively. The inset shows remanences M_R.

helps to isolate the magnetic particles and quenches the remanence.

The magnetization M due to a classical elemental moment μ is described by a Langevin function[10] $L(a) = \coth a - 1/a$,

$$M = \mu N L\left(\frac{\mu H}{kT}\right),$$

where k is the Boltzmann's constant and N number of the elemental moments. Fits of the experimental M vs H/T curves with this formula were, however, unsuccessful as shown in Fig. 3 with a dashed curve. Since there is a distribution of particle sizes and, consequently of μ, a fit was attempted with the following formula,

$$M = \mu_1 N_1 L\left(\frac{\mu_1 H}{kT}\right) + \mu_2 N_2 L\left(\frac{\mu_2 H}{kT}\right).$$

The results obtained with a nonlinear least-squares fit are included in Fig. 3 as solid curves, showing excellent agreements with the plots. The values of μ_1, N_1, μ_2, N_2 should be regarded as representaives of a range of real values, though without clear physical meaning by themselves. In Table III, the values are listed and compared with ${}^{\mathrm{tem}}\mu$, which is the expected moment of the average grain observed by TEM assuming spherical γ-Fe_2O_3 grains. It should be noted that μ_1 and μ_2, even the larger one, are far smaller, by one or two orders of magnitude, than ${}^{\mathrm{tem}}\mu$. The saturation magnetization determined by the fitting ${}^{\mathrm{fit}}\sigma_s = \mu_1 N_1 + \mu_2 N_2$ is, however, comparable with ${}^{\mathrm{cal}}\sigma_s$ calculated from the iron concentration of 40 at% measured by RBS. The difference ${}^{\mathrm{fit}}\sigma_s/{}^{\mathrm{cal}}\sigma_s \sim 0.5$ is tolerable taking into account the nanostructures of the present sample. These facts indicate that the magnetization measured in the present samples originates from some structures smaller than the size observed by TEM.

The values of μ_1, N_1, μ_2, N_2 are shown in Fig. 4 as a plot of μN vs μ. Each set of points can be regarded as a representative of the size distribution of the magnetic moment, as described above, and serves as an indicator for estimating annealing effects on the distribution. The figure indicates that the O_2-annealing process drastically changes the size and relative frequency of the moments; the smaller moments are not altered by the annealing process in an oxidizing atmosphere, while the larger moments are decreased both in their effective size and frequency.

4. Summary

We have demonstrated the sysnthesis of a magnetic nanocomposite composed of silver and iron oxide, mainly γ-Fe_2O_3, by the inert gas condensation process combined with *in situ* oxidation. The as-prepared material contains an amount of non-equilibrium iron in the silver matrix which are magnetically activated by an inert heat treatment. An oxidizing heat treatment can modify the magnetic properties forming an antiferromagnetic phase of α-Fe_2O_3, surrounding and isolating magnetic grains. By optimizing the conditions of the heat treatment and iron content in the composite, this process promises to be of use in synthesizing practical magnetic nanocomposites.

Table III. Magnetic moments μ and saturation magnetizations σ_s in Ag/FeO_x nanocomposite containing 40 at% iron.

	Unit	As-compacted	He-annealed	O_2-annealed
TEM results				
Grain size	nm	15	20	20
${}^{\mathrm{tem}}\mu$	μ_B	7.8×10^4	1.8×10^5	1.8×10^5
${}^{\mathrm{cal}}\sigma_s$	emu/g	27	27	27
Fitting results				
μ_1	μ_B	1.8×10^4	1.8×10^4	6.5×10^3
μ_2	μ_B	1.4×10^3	1.4×10^3	9.6×10^2
${}^{\mathrm{fit}}\sigma_s$	emu/g	12	13	6.8

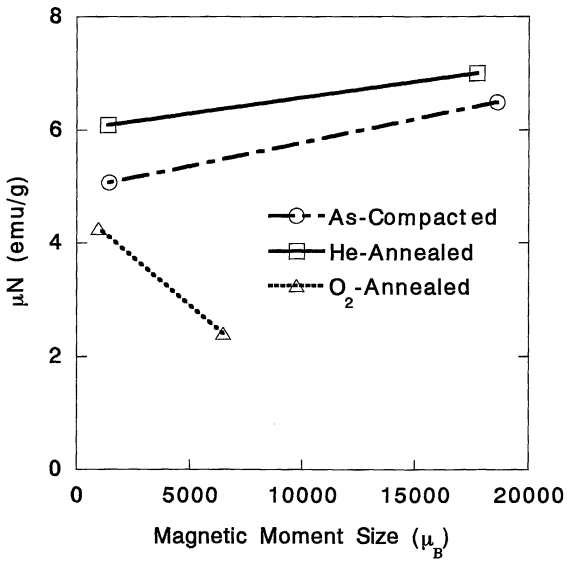

Fig. 4. Annealing effects on the effective magnetic moment size in Ag/FeO_x nanocomposites containing 40 at% iron. The values of μ and N are, respectively, an effective size of the magnetic moment and its frequency determined by fits assuming a bimodal Langevin function.

Acknowledgement

The authors thank prof. M. C. Croft (R. Univ.) for XAS measurements, and R. Krawchuk (R. Univ.) for RBS.

1) C. L. Chien: J. Appl. Phys. **69** (1991) 5267.
2) R. Dagani: Chem. & Eng. News, Nov. 23 (1992) 18.
3) A. E. Berkowitz, J. R. Michell, M. J. Carey, A. P. Young, S. Zhang, F. E. Spada, F. T. Parker, A. Hutten and G. Thomas: Phys. Rev. Lett. **68** (1992) 3745.
4) G. Xiao, J. Q. Wang and P. Xiong: Appl. Phys. Lett. **62** (1993) 420.
5) C. L. Chien, J. Q. Xiao and J. S. Jiang: J. Appl. Phys. **73** (1993) 5309.
6) R. D. Shull, L. J. Swartzendruber and L. H. Bennet: *Proc. 6th Int. Cryocoolers Conf.*, eds. G. Green and M. Knox (David Tayler Res. Cntr. Publ., #DTRC-91/002, Annapolis, 1991) p.231.
7) R. D. Shull and L. H. Bennet: NanoStructured Mater. **1** (1992) 83.
8) R. D. McMichael, R. D. Shull, L. J. Swartzendruber and L. H. Bennet: J. Mag. Mag. Mater. **111** (1992) 29.
9) R. Birringer, U. Herr and H. Gleiter: Trans. Jpn. Inst. Met. **27** (1987) 43.
10) C. P. Bean and J. D. Livingston: J. Appl. Phys., Suppl. **30** (1959) 120S.